Adsorption of Cationic Dye from Aqueous Solution by Clay as an Adsorbent: Thermodynamic and Kinetic Studies

[1]BAYBARS ALI FİL* AND [2]CENGIZ OZMETİN**
[1]*Ataturk University*, *Faculty of Engineering*, *Department of Environmental Engineering*, *25240*, *Erzurum, Turkey.*
[2]*Balikesir University*, *Faculty of Engineering - Architecture*, *Department of Environmental Engineering*, *10145*, *Balikesir, Turkey.*
baybarsalifil2@gmail.com*, cozmetin1@yahoo.com**

(Received on 4th January 2012, accepted in revised form 7th January 2012)

Summary: In the study, montmorillonite was used as an adsorbent for the removal of methylene blue (MB) from aqueous solutions. Batch studies were performed to address various experimental parameters like contact time, pH, temperature, stirring speed, ionic strength, adsorbent dosage and initial concentration for the removal of this dye. Adsorption rate increased with the increase in initial dye concentration, ionic strength, stirring speed, pH and temperature. Kinetic study showed that the adsorption of dye on montmorillonite was a gradual process. Quasi-equilibrium reached in 3 h. Pseudo-first-order, pseudo-second-order, Elovich, Bangham, mass transfer and intra-particle particle diffusion models were used to fit the experimental data. Pseudo-second-order rate equation was able to provide realistic description of adsorption kinetics. Intra-particle diffusion process was identified as the main mechanism controlling the rate of the dye sorption. The diffusion coefficient, *D*, was found to increase when the stirring speed, ionic strength and temperature were raised. Thermodynamic activation parameters such as ΔG^*, ΔS^* and ΔH^* were also calculated.

Keywords: Montmorillonite; Dyes; Adsorption; Adsorption kinetics; Activation parameters; Thermodynamics.

Introduction

Dyes are synthetic organic compounds that are increasingly being produced and used as colorants in many industries worldwide, including textile, plastic, paper, etc. [1, 2]. Most of the dyes are toxic and carcinogenic compounds; they are also recalcitrant and thus stable in the receiving environment, posing a serious threat to human and environmental health. Accordingly, to protect humans and the receiving ecosystem from contamination, the dyes must be eliminated from the dye-contained wastewaters before being released into the environment. Because dye molecules are resistant to biodegradation [3], biological processes are not useful or efficient methods for the removal of dyes from effluent.

Dyes are usually stable to photo-degradation, bio-degradation and oxidizing agents [4], which led to intensive investigations on physical or chemical methods to remove color from textile effluent. These studies include the use of coagulants [5], ultra-filtration [6] and electro-chemical [7, 8]. The advantages and disadvantages of each technique have been extensively reviewed [9].

One of the conventional methods for removal of dyes from wastewater is adsorption [10-13]. The adsorption process provides an attractive alternative treatment, especially if the adsorbent is inexpensive and readily available. Activated carbon is popular and an effective dye sorbent, but its relatively high price, high operating costs and problems with regeneration hamper its large-scale application. Therefore, there is a growing need in finding low cost, renewable, locally available materials as sorbent for the removal of dye colors [14-16].

A large variety of non-conventional adsorbent materials have been also proposed and studied for their ability to remove dyes [1]. Therefore, in recent years, many investigators have studied the feasibility of using low cost substances, such as: plum kernels [17], chitin [18] ,chitosan [19], perlite [20], natural clay [21, 22], bagasse pith [23], fly ash [24, 25], wood [26, 27], rice husk [28] and peat [29, 30].

The aim of this study is to further explore the application of montmorillonite for dye adsorption and to investigate the kinetics and mechanism involved in dye adsorption on montmorillonite. Therefore, the dynamical behaviors of adsorption were measured on the effect of contact time, agitation speed, ionic strength, adsorbent dosage, pH and temperature. The adsorption rates were determined quantitatively and simulated by the Elovich, the pseudo-first-order and second-order models, and then adsorption mechanism was analyzed using mass transfer coefficient. Bangham's equation and intra-particle diffusion, Furthermore, thermodynamic activation parameters were also determined.

*To whom all correspondence should be addressed.

Results and Discussion

Adsorption Rate

Adsorption rate was investigated using the values of dye adsorbed at different initial dye concentrations, stirring speeds, adsorbent dosages, ionic strengths, temperatures and pHs as a function of reaction time.

Effect of Initial pH Solution

The surface adsorption rate of methylene blue on montmorillonite was investigated in pH range of 5 – 11 at 303 K, 0.3 g L^{-1} adsorbent dosage and 200 rpm stirring speed. The studies were carried out for 3 h. Initial dye concentration was $1.0x10^{-4}$ mol L^{-1}. Fig. 1 showed the effect of pH on the removal rate of MB on montmorillonite. The adsorption of MB by montmorillonite was increased with increase in pH. This can be explained by considering the pHiep of montmorillonite. As pH of the system decreased below the pHiep of the adsorbent, the number of negatively charged adsorbent sites decreased and the positively charged surface sites increased, which did not favor the adsorption of cationic dyes due to electrostatic repulsion. At higher pH, negatively charged adsorbent sites increased, which enhances the adsorption of positively charged dye cations through electrostatic forces of attraction [31].

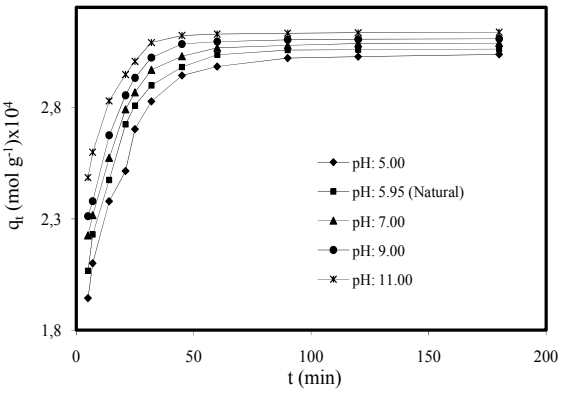

Fig. 1: Effect of solution pH on dye adsorption on montmorillonite (Conditions: initial MB 1.0×10^{-4} mol L^{-1}. adsorbent dosage 0.3 g L^{-1}, temperature 303 K, stirring speed 200 rpm, ionic strength 0 mol L^{-1} NaCl).

Effect of Ionic Strength

The presence of co-ions in solution can affect the sorption of MB. The effect of salt concentration (ionic strength) on the amount of dye sorbed by the clay was analyzed over the NaCl concentration ranging from 0 to $0.1x10^{-1}$ mol L^{-1} and the results were shown in Fig. 2. As seen in Fig. 2, the presences of NaCl significantly affected the absorption rate of dye. The presence of NaCl in the solution may have two opposite effects. On the one hand, since the salt screens the electrostatic interaction of opposite changed of the oxide surface and the dye molecules, the adsorbed amount should decreased with increasing of NaCl concentration. On the other hand, the salt causes an increase in the degree of dissociation of the dye molecules by facilitating the protonation [12, 29, 32].

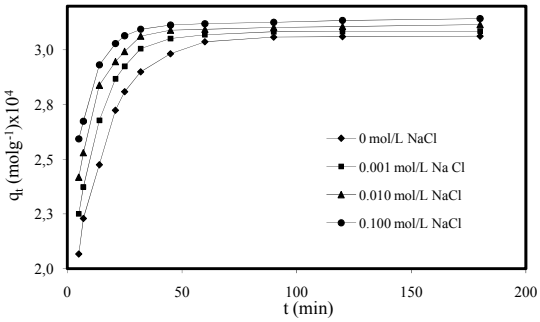

Fig. 2: Effect of ionic strength on dye adsorption on montmorillonite (Conditions: initial MB 1.0×10^{-4} mol L^{1}, adsorbent dosage 0.3 g L^{-1}, temperature 303 K, stirring speed 200 rpm, solution pH 5.95 (Natural)).

Effect of Stirring Speed

The variation of adsorption of methylene blue dyes by montmorillonite stirring speed range (100 – 400 rpm) at an initial dye concentration of $1.0x10^{-4}$ mol L^{-1}, a temperature of 303 K and natural pH was shown in Fig. 3. In the batch adsorption systems, agitation speed plays a significant role in affecting the external boundary film and the distribution of the solute in the bulk solution [33]. The results showed that the adsorption rate of MB almost remained unchanged as agitation speed was increased. A similar trend was observed for varying agitation speeds at different times. These observations can be explained by the fact that the boundary layer resistance was very small and the mobility of the system was high under the experimental conditions. In other words, the diffusion of the MB ion from the solution to the surface of the montmorillonite and into the pores occurred quickly and easily. Since the uptake of MB was not significantly influenced by the degree of agitation. Therefore an agitation speed of 200 rpm was used for all further experiments.

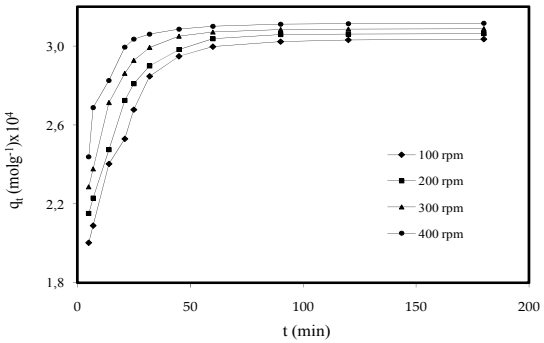

Fig. 3: Effect of stirring speed on dye adsorption on montmorillonite (Conditions: initial MB 1.0×10^{-4} mol L^{-1}, adsorbent dosage 0.3 g L^{-1}, temperature 303 K, ionic strength: 0 mol L^{-1} NaCl, solution pH 5.95 (Natural))

Effect of Initial Dye Concentration

The influence of initial dye concentration on the MB adsorption kinetic was studied with a series of experiments at different MB concentrations (1.0×10^{-4} – 3.0×10^{-4} mol L^{-1}). The results showed that the amount of MB adsorbed increased as the dye concentration increased (Fig. 4). Results showed that increased initial MB concentration led to increased MB adsorption. Apparently, the initial MB concentration plays an important role in affecting the capacity of MB to absorb onto montmorillonite. The higher the MB concentration is, the stronger the driving forces of the concentration gradient, and therefore the higher the adsorption capacity [34].

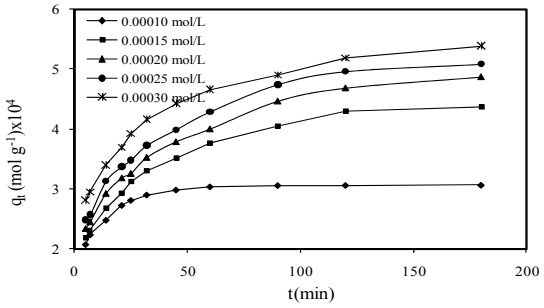

Fig. 4: Effect of initial dye concentration on dye adsorption on montmorillonite (Conditions: stirring speed 200 rpm, adsorbent dosage 0.3 g L^{-1}, temperature 303 K, ionic strength 0 mol L^{-1} NaCl, solution pH 5.95 (Natural))

Effect of Adsorbent Dosage

The sorbent mass was varied from 0.1 to 0.4 g L^{-1} keeping the MB concentration constant (1.0×10^{-4} mol L^{-1}) and the results were shown in Fig. 5. The percentage of MB sorption increased with the increase of sorbent amount from 0.1 to 0.4 g L^{-1} but the uptake capacity of the adsorbent decreased from. This may be attributed to the availability of more sorption sites due to higher amount of the sorbent. At higher montmorillonite to solute ratios, there is a very fast sorption onto the sorbent surface that produces a lower solute concentration in the solution compared to the sorbent to solute concentration ratio is lower [35].

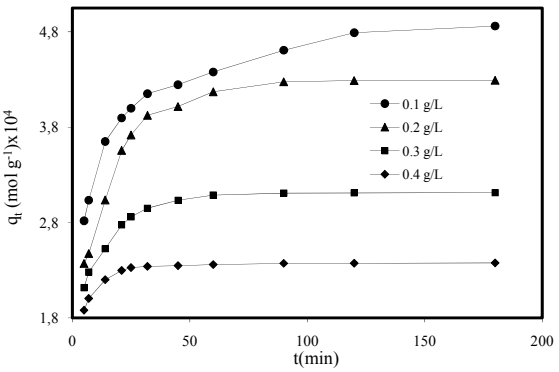

Fig. 5: Effect of adsorbent dosage on dye adsorption on montmorillonite (Conditions: initial MB 1.0×10^{-4} mol L^{-1}, stirring speed 200 rpm, temperature 303 K, ionic strength 0 mol L^{-1} NaCl, solution pH 5.95 (Natural))

Effect of Temperature

It has been believed that the temperature generally has two major effects on the adsorption process. Increasing the temperature will increase the rate of diffusion of the adsorbate molecules across the external boundary layer and in the internal pores of the adsorbent particle, owing to the decrease in the viscosity of the solution. In addition, changing the temperature will change the equilibrium capacity of the adsorbent for a particular adsorbate [36]. Fig. 6 showed the effect of temperature on dynamic adsorption of MB on montmorillonite. It was seen that higher temperature will result in an increase in dye adsorption on montmorillonite, suggesting that the dye adsorption is an endothermic process. The temperature seems to have a significant effect on MB adsorption.

Adsorption Kinetics

The kinetics of adsorption data was processed to understand the dynamics of adsorption process in terms of the order of rate constant. Three kinetic models were applied to the adsorption kinetic data in order to investigate the behavior of adsorption process of methylene blue onto montmorillonite. These models are the Elovich, the pseudo-first-order and pseudo-second order models.

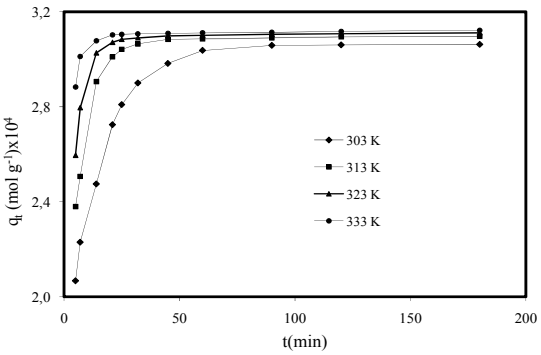

Fig. 6: Effect of temperature on dye adsorption on montmorillonite (Conditions: initial MB 1.0×10^{-4} mol L^{-1}, stirring speed 200 rpm, ionic strength 0 mol L^{-1} NaCl, solution pH 5.95 (Natural)).

The Elovich Equation

The Elovich model equation is generally expressed as

$$\frac{dq_t}{dt} = \alpha \exp\left(-\beta q_t\right) \qquad (2)$$

To simplify the Elovich, [37] αβ>t and by applying the boundary conditions q_t=0 at t=0 and q_t=q_t at t=t, Eq(2) becomes

$$q_t = \frac{1}{\beta}\ln\left(\alpha\beta\right) + \frac{1}{\beta}\ln t \qquad (3)$$

The plot of q_t versus *ln t* should yield a linear relationship with a slope *1/β* and an intercept of *1/β ln(αβ)*. The *α* initial adsorption rate (mol g^{-1} min^{-1}) and *β* desorption constant (g mol^{-1}) values, the correlation coefficients. R^2, were given in Table-1. From these mechanisms, it was observed that the Elovich kinetic model did not adequately fit the experimental values ($0.8205 < R^2 < 0.9896$).

Pseudo-first-order Kinetic Model

The rate constant of adsorption is determined from the first-order rate expression given by Lagergren and Svenska [38]. which is the earliest known equation describing the adsorption rate based on the adsorption capacity. The differential equation is generally expresses a follows:

$$\frac{dq_t}{dt} = k_1\left(q_e - q_t\right) \qquad (4)$$

where k_1 is the rate constant of pseudo-first-order adsorption and q_e represents adsorption capacity (i.e. the amount of adsorption corresponding to monolayer coverage). After definite integration by applying the initial conditions $t = 0$ to t and $q_t = 0$ to q_t Eq. (4) becomes:

$$\ln\left(q_e - q_t\right) = \ln q_e - k_1 t \qquad (5)$$

where q_e and q_t are the amount of dye adsorbed (mol g^{-1}) at equilibrium and at any time t, k_1 is the rate constant (min^{-1}). The plot of *ln (qe − qt)* versus *t* gives a straight line for the pseudo-first-order adsorption kinetics. The values of the pseudo-first-order rate constant k_1 were obtained from the slopes of the straight lines. The k_1 values, the correlation coefficients, R^2, were given in Table-1. From this table, it has been seen that while pseudo-first-order kinetic model was not fit very well ($0.6512 < R^2 < 0.9694$).

Pseudo-second-order Kinetic Model

Adsorption kinetics was explained by the pseudo-second-order model developed by [39]:

$$\frac{dq_t}{dt} = k_2\left(q_e - q_t\right)^2 \qquad (6)$$

Integrating this equation for the boundary condition (t = 0 to t and q_t = 0 to q_t), gives:

$$\frac{t}{q_t} = \left[\frac{1}{k_2 q_e^{\,2}}\right] + \frac{1}{q_e}t \qquad (7)$$

Where k_2 is the equilibrium rate constant of pseudo-second-order equation (g mol^{-1} min^{-1}) and $h=k_2qe^2$ is initial adsorption rate (mol g^{-1} min^{-1}). If the second-order kinetics is applicable, then the plot of *t/qt* versus *t* should show a linear relationship. There is no need to know any parameter beforehand and the equilibrium adsorption capacity, *q*e, can be calculated from Eq. (7). Also, it is more likely to predict the behavior over the whole range of adsorption. Values of k_2 and *q*e were calculated from the intercept and slope of the plots of *t*/*qt* versus *t*. The linear plots of *t*/*qt* versus *t* (Fig. 7) showed a good agreement between experimental. The correlation coefficients (R^2) were 0.9912 – 1.0000 (Table-1), suggested a strong relationship between the parameters and also explained that the process followed pseudo-second-order kinetics. Kinetics of MB adsorption on montmorillonite followed the pseudo second order model, suggesting that the rate-limiting step may be chemisorptions [40, 41]. This confirmed that adsorption of dye took place probably via surface exchange reactions until the surface functional sites were fully occupied; thereafter dye molecules diffused into the polymer network for further

interactions (such as inclusion complex, hydrogen bonding, hydrophobic interactions). Similar results were obtained in the methylene blue adsorption onto clay [42], cationic dyes (methylene blue, crystal violet) adsorption to palygorskite [43], cationic dyes (Basic Blue 3, Basic Violet 3) adsorption onto a cyclodextrin polymer [11], cationic dyes (Basic Yellow 28, Methylene Blue, Malachite Green) adsorption onto Persian Kaolin [44] and cationic dyes (methylene blue, methyl violet) adsorption onto sepiolite [12].

The half-adsorption time of the dye, $t_{1/2}$, i.e. the time required for the montmorillonite to uptake half of the amount adsorbed at equilibrium, is often considered as a measure of the rate of adsorption and for the second-order process is given by the relationship [45]:

$$t_{1/2} = \frac{1}{k_2 q_e} \qquad (8)$$

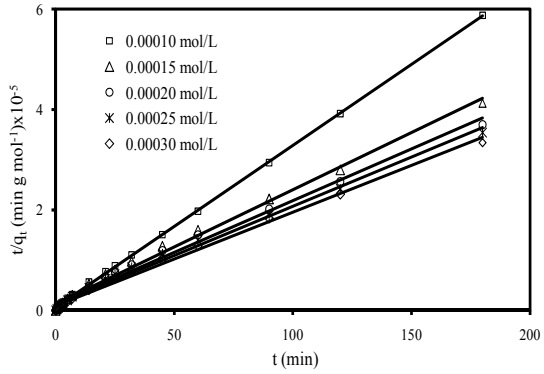

Fig. 7: Second-order kinetic equation for adsorption of methylene blue on montmorillonite at different initial dye concentrations (Conditions: stirring speed 200 rpm, adsorbent dosage 0.3 g L^{-1}, temperature 303 K, ionic strength 0 mol L^{-1} NaCl, solution pH 5.95 (Natural)).

The determined values of $t_{1/2}$ for the tested parameters were given in Table-1.

Adsorption Mechanism

The removal of methylene blue by adsorption on montmorillonite was found to be rapid at the initial period of contact time and then to become slow and stagnate with the increase in contact time. The removal of methylene blue by adsorption on surface of montmorillonite was due to MB as MB^+ cationic form. The mechanism for the removal of dye by adsorption may be assumed to involve the following three steps.

The adsorption process of the adsorbate molecules from the bulk liquid phase onto the adsorbent surface is presumed to involve three stages: (1) mass transfer of the adsorbate molecules across the external boundary layer; (2) intraparticle diffusion within the pores of the adsorbent; (3) adsorption at a site on the surface.

Mass transfer coefficient

Mass transfer coefficients, β_L (m s^{-1}) of methylene blue at the montmorillonite-solution interface, were determined by using the Eq. (9) [46]:

$$\ln\left(\frac{C_0}{C_t} - \frac{1}{1+mK}\right) = \ln\left(\frac{mK}{1+mK}\right) - \left(\frac{1+mK}{mK}\right)\beta_L S_S t \qquad (9)$$

where K is the adsorption constant (L mol^{-1}), m is the weight of adsorbent per liter of solution (g L^{-1}) and S_S is the surface area of adsorbent (m^2 g^{-1}). A linear graphical relation between $ln[(Ct/C0)-1/(1+ mK)]$ versus t was not obtained. In plotting the curves, K value for the adsorption of methylene blue onto montmorillonite was calculated. This result indicated that the model mentioned above for the system was not validity. The correlation coefficients, R^2, calculated from equation mentioned above were given in Table-2.

Bangham's Equation

Kinetic data can further be used to check whether film diffusion is the only rate-controlling step or not in the adsorption system using Bangham's equation [47]:

$$\log\log\left(\frac{C_0}{C_0 - q_t m}\right) = \log\left(\frac{k_{0B} m}{2,303V}\right) + \alpha_B \log(t) \qquad (10)$$

where C_0 is the initial concentration of adsorbate in solution (mol L^{-1}), V is the volume of solution (ml), m is the weight of adsorbent per liter of solution (g L^{-1}), q_t (mol g^{-1}) is the amount of adsorbate retained at time t, and α_B (less than 1) and k_{0B} are constants (ml g^{-1} L) (Table-2). The double logarithmic plot did not yield satisfactory linear curves for the removal of MB onto montmorillonite ($0.857 < R^2 < 0.983$). This showed that the film diffusion was not the only rate controlling parameter. It may be concluded that the film and pores diffusion were important to different extents in the removal process [48].

Table-1: The comparison of the Elovich, first-order and second-order rate constant and correlation coefficients at different conditions.

Parameters						Kinetic Models								
						The Elovich Equation			Pseudo – first – order		Pseudo – second – order			
Adsorbent dosage (g.L-1)	Temperature (K)	Initial dye concentration (x10-4 mol L-1)	pH	Stirring speed (rpm)	Ionic strength (mol L-1)	R^2	α mol g^{-1}min-1 ($x10^4$)	β g mol^{-1} ($x10^4$)	R^2	k_1 min^{-1}	$h=k_2xqe^2$ $x10^5$ mol g^{-1} min^{-1}	k_2 .g mol^{-1} min^{-1}	R^2	$t_{1/2}$. min
0.30	303	1.00	5.95	100	0	0.9630	51.747	3.202	0.9292	0.0540	14.992	1589.705	0.9994	2.048
0.30	303	1.00	5.95	200	0	0.9684	27.327	2.857	0.9421	0.0621	17.125	1784.016	0.9997	1.809
0.30	303	1.00	5.95	300	0	0.9314	42.536	2.951	0.9136	0.0629	22.235	2286.507	0.9999	1.402
0.30	303	1.00	5.95	400	0	0.9145	298.711	3.579	0.8713	0.0609	35.073	3569.059	0.9999	0.894
0.30	303	1.00	5.95	200	0	0.9684	27.327	2.857	0.9421	0.0621	17.125	1784.016	0.9997	1.809
0.30	303	1.50	5.95	200	0	0.9660	13.794	1.988	0.9677	0.0207	8.080	419.894	0.9938	5.429
0.30	303	2.00	5.95	200	0	0.9425	15.276	1.837	0.9694	0.0174	8.036	341.148	0.9912	6.040
0.30	303	2.50	5.95	200	0	0.9389	67.030	1.925	0.9614	0.0179	8.923	343.171	0.9922	5.715
0.30	303	3.00	5.95	200	0	0.8984	55.990	1.817	0.9451	0.0161	10.924	379.825	0.9945	4.909
0.30	303	1.00	5.00	200	0	0.9556	57.987	3.258	0.8996	0.0479	14.586	1544.416	0.9994	2.107
0.30	303	1.00	5.95	200	0	0.9684	27.327	2.857	0.9421	0.0621	17.125	1784.016	0.9997	1.809
0.30	303	1.00	7.00	200	0	0.9519	35.217	2.910	0.9245	0.0595	19.089	1957.005	0.9998	1.636
0.30	303	1.00	9.00	200	0	0.9466	97.955	3.245	0.9031	0.0633	24.008	2439.085	0.9998	1.307
0.30	303	1.00	11.00	200	0	0.9440	804.432	3.905	0.8665	0.0624	34.681	3476.297	0.9999	0.911
0.30	303	1.00	5.95	200	0	0.9684	27.327	2.857	0.9421	0.0621	17.125	1784.016	0.9997	1.809
0.30	303	1.00	5.95	200	$1x10^{-3}$	0.9429	80.463	3.194	0.9112	0.0637	23.853	2460.008	0.9999	1.305
0.30	303	1.00	5.95	200	$1x10^{-2}$	0.9310	306.860	3.617	0.7932	0.0506	31.656	3223.122	0.9999	0.990
0.30	303	1.00	5.95	200	$1x10^{-1}$	0.9078	400.767	3.646	0.7561	0.0486	37.617	3772.428	1.0000	0.839
0.30	303	1.00	5.95	200	0	0.9684	27.327	2.857	0.9421	0.0621	17.125	1784.016	0.9997	1.809
0.30	313	1.00	5.95	200	0	0.9227	386.703	3.693	0.8556	0.0595	37.536	3867.760	0.9999	0.830
0.30	323	1.00	5.95	200	0	0.8863	1392.233	4.083	0.7484	0.0541	53.885	5521.630	1.0000	0.580
0.30	333	1.00	5.95	200	0	0.8205	72619.860	5.388	0.6512	0.0487	94.545	9665.054	1.0000	0.331
0.10	303	1.00	5.95	200	0	0.9896	15.782	1.704	0.7788	0.0318	13.730	589.212	0.9981	3.516
0.20	303	1.00	5.95	200	0	0.9677	8.076	1.701	0.9598	0.0580	13.355	714.325	0.9990	3.238
0.30	303	1.00	5.95	200	0	0.9684	27.327	2.857	0.9421	0.0621	17.125	1784.016	0.9997	1.809
0.40	303	1.00	5.95	200	0	0.9132	236.843	4.822	0.8244	0.0551	26.744	4889.765	1.0000	0.874

Intra-particle Diffusion Model

The intraparticle diffusion model proposed by Furusawa and Smith [49] is applied to study the adsorption process, which is written as:

$$q_t = k_{dif} t^{1/2} + C \qquad (11)$$

where q_t (mol g^{-1}) is the amount of solute on the surface of the sorbent at time t, k_{dif} is the intraparticle diffusion rate constant (mol g^{-1} $min^{-1/2}$) and C is the intercept (mol g^{-1}) and it gives an idea of the thickness of the boundary layer. The k_{dif} values are found from the slopes of q_t versus $t^{1/2}$ plots. If the intraparticle diffusion is involved in the adsorption process, then the plot of the square root of time versus the uptake (q_t) would result in a linear relationship, and the intraparticle diffusion would be the controlling step if this line passed through the origin. When the plots do not pass through the origin, this is indicative of some degree of boundary layer control and these further shows that the intraparticle diffusion is not the only rate controlling step, but also other processes may control the rate of adsorption.

The k_{dif} values were calculated by using correlation analysis (Table-2). The correlation coefficients, R^2 are close to unity indicating the application of this model. This functional relationship corresponds to the characteristic of intra-particle diffusion. The intra-particle diffusion plots have been given in Fig. 8. The values of intercept give an idea about the boundary layer thickness. i.e., the larger intercept the greater is the boundary layer effect [12]. The applicability of intra-particle diffusion model indicates that it is the rate-determining step. Similar results were obtained for basic red 22 on pith [50] and methylene blue on perlite [20].

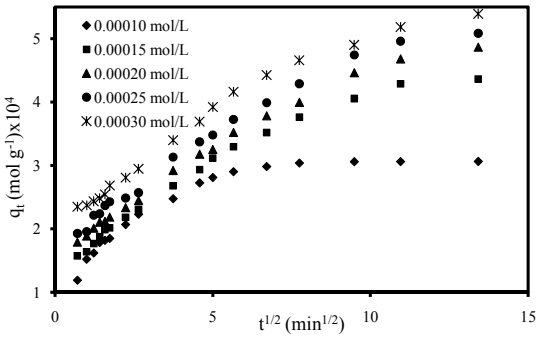

Fig. 8: Intra-particle diffusion plots for adsorption of methylene blue on montmorillonite at different initial dye concentrations (Conditions: stirring speed 200 rpm, adsorbent dosage 0.3 g L^{-1}, temperature 303 K, ionic strength 0 mol L^{-1} NaCl, solution pH 5.95 (Natural)).

Table-2: Adsorption mechanism for methylene blue onto montmorillonite.

Parameters						Adsorption mechanism									
						Mass transfer coefficient		Intra-particle diffusion model				Bangham's equation			Diffusion coefficient
Adsorbent dosage (g.L^{-1})	Temperature (K)	Concentration (x10^4 mol	pH	Stirring speed (rpm)	Ionic strength (mol L^{-1})	β_L x10^4	R^2	$k_{i,1}$x10^6	R^2	$k_{i,2}$x10^7	R^2	α_B	k_{0B}	R^2	D (cm^2.s^{-1}) x10^9
0.30	303	1.00	5.95	100	0	14.16	0.663	25.43	0.986	18.90	0.938	0.281	2.138	0.964	2.780
0.30	303	1.00	5.95	200	0	15.56	0.628	30.29	0.973	11.30	0.955	0.320	1.989	0.978	3.148
0.30	303	1.00	5.95	300	0	17.77	0.567	29.56	0.987	9.80	0.972	0.313	2.202	0.948	4.061
0.30	303	1.00	5.95	400	0	20.94	0.506	27.50	0.979	6.10	0.970	0.269	2.863	0.939	6.372
0.30	303	1.00	5.95	200	0	15.56	0.628	30.29	0.973	11.30	0.955	0.320	1.989	0.978	3.148
0.30	303	1.50	5.95	200	0	8.54	0.863	35.32	0.995	151.30	0.988	0.295	1.390	0.971	1.049
0.30	303	2.00	5.95	200	0	4.43	0.824	34.93	0.997	200.80	0.996	0.250	1.120	0.967	0.943
0.30	303	2.50	5.95	200	0	3.16	0.728	33.93	0.989	193.40	0.997	0.191	1.243	0.965	0.997
0.30	303	3.00	5.95	200	0	2.40	0.733	31.56	0.993	233.70	0.995	0.185	1.017	0.965	1.160
0.30	303	1.00	5.00	200	0	14.11	0.672	28.65	0.985	4.00	0.965	0.276	2.163	0.957	2.703
0.30	303	1.00	5.95	200	0	15.56	0.628	30.29	0.973	11.30	0.955	0.320	1.989	0.978	3.148
0.30	303	1.00	7.00	200	0	17.15	0.609	30.26	0.991	10.10	0.945	0.317	2.112	0.965	3.481
0.30	303	1.00	9.00	200	0	19.11	0.579	28.00	0.979	3.10	0.960	0.291	2.470	0.959	4.358
0.30	303	1.00	11.00	200	0	22.75	0.541	23.97	0.961	2.00	0.972	0.251	3.129	0.958	6.254
0.30	303	1.00	5.95	200	0	15.56	0.628	30.29	0.973	11.30	0.955	0.320	1.989	0.978	3.148
0.30	303	1.00	5.95	200	1 x10^{-3}	19.20	0.566	30.23	0.969	2.60	0.976	0.291	2.399	0.956	4.363
0.30	303	1.00	5.95	200	1 x10^{-2}	20.33	0.530	27.25	0.947	3.10	0.946	0.266	2.837	0.949	5.753
0.30	303	1.00	5.95	200	1x10^{-1}	22.94	0.499	26.20	0.957	5.10	0.979	0.270	2.983	0.935	6.785
0.30	303	1.00	5.95	200	0	15.56	0.628	30.29	0.973	11.30	0.955	0.320	1.989	0.978	3.148
0.30	313	1.00	5.95	200	0	20.02	0.477	28.12	0.968	2.00	0.976	0.260	2.916	0.935	6.862
0.30	323	1.00	5.95	200	0	21.95	0.416	41.39	0.989	3.00	0.986	0.242	3.318	0.906	9.824
0.30	333	1.00	5.95	200	0	23.84	0.338	50.91	0.991	2.00	0.986	0.194	4.212	0.857	17.216
0.10	303	1.00	5.95	200	0	1.72	0.594	42.08	0.991	122.20	0.956	0.230	0.743	0.983	1.620
0.20	303	1.00	5.95	200	0	8.94	0.670	31.56	0.990	124.90	0.981	0.350	1.260	0.976	1.759
0.30	303	1.00	5.95	200	0	15.56	0.628	30.29	0.973	11.30	0.955	0.320	1.989	0.978	3.148
0.40	303	1.00	5.95	200	0	81.02	0.492	20.62	0.971	4.10	0.953	0.264	6.956	0.935	6.513

Diffusion Coefficient

The values of diffusion coefficient largely depend on the surface properties of adsorbents. The diffusion coefficients for the intra-particle transport of methylene blue within the pores of montmorillonite particles have been calculated at different temperatures, stirring speed, ionic strength, initial dye concentrations and pH by employing the Eq. (12) [20, 51]:

$$t_{1/2} = \frac{0,030\, r_0^2}{D} \qquad (12)$$

where D is the diffusion coefficient with the unit cm^2 s^{-1}; $t_{1/2}$ is the time, min, for half adsorption of methylene blue and r_0 is the radius of the adsorbent particle in cm. The value of r_0 was calculated as 3.375×10^{-3} cm for montmorillonite sample. For the present study, the pore diffusion coefficient values obtained from Eq. (12) were given in Table-2. The values of diffusion coefficient for adsorption of methylene blue were found to vary between 0.943x10^{-9} cm^2 s^{-1} to 17.216x10^{-9} cm^2 s^{-1}. Diffusion coefficient values are affected by many factors such as dye molecular weight, structure; functional groups have in the type and amount of adsorbent materials used electrokinetic surface properties.

Activation Energy

Adsorption rate constant temperature dependence can be given as follows [52, 53]:

$$\ln k_2 = \ln k_0 - \frac{E_a}{R_g}\frac{1}{T} \qquad (13)$$

where k_2 is the pseudo-second-order constant (g mol^{-1} min^{-1}), k_0 is the rate constant of adsorption (g mol^{-1} min^{-1}), E_a is activation energy of adsorption (kJ mol^{-1}), R_g is the gas constant (8.314 J mol^{-1} K^{-1}), T is the solution temperature (K). Plotting of $\ln k_2$ against the reciprocal temperature gives a reasonably straight line, the gradient of which is $-E_a/R_g$. From Eq, (13), the activation energy, E_a, was 45.597 kJ mol^{-1} (Fig. 9). The magnitude of activation energy gave an idea about the type of adsorption which is mainly physical or chemical. Low activation energies (5–50 kJ mol^{-1}) are characteristics for physical adsorption, while higher activation energies (60–800 kJ mol^{-1}) suggest chemical adsorption [54].

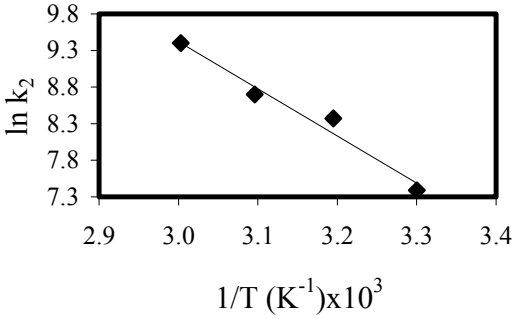

Fig. 9: Arrhenius plots for adsorption of dye on montmorillonite. (Conditions: initial MB 1.0×10^{-4} mol L^{-1}, stirring speed 200 rpm, ionic strength 0 mol L^{-1} NaCl, solution pH 5.95 (Natural)).

Thermodynamic Parameters

Free energy (ΔG^*), enthalpy (ΔH^*) and entropy (ΔS^*) of activation can be calculated by Eyring equation [55]:

$$\ln\left(\frac{k_2}{T}\right)=\left[\left(\frac{k_b}{h}\right)+\frac{\Delta S^*}{R_g}\right]-\frac{\Delta H^*}{R_g}\frac{1}{T} \quad (14)$$

where k_b and h are Boltzmann's and Planck's constants, respectively. According to Eq. (14), a plot of ln(k/T) versus 1/T should be a straight line with a slope $\Delta H^*/R_g$ and intercept $[ln(k_b/h)+\Delta S^*/R_g]$. ΔH^* and ΔS^* were calculated from slope and intercept of line, respectively (Fig. 10). Gibbs energy of activation may be written in terms of entropy and enthalpy of activation:

$$\Delta G^* = \Delta H^* - T.\Delta S^* \quad (15)$$

ΔG^* was calculated at 303 K from Eq. (15). It was found that the values of the free energy (ΔG^*), enthalpy (ΔH^*) and entropy (ΔS^*) of activation were 47.587 kJ mol^{-1}, 42.884 kJ mol^{-1} and −0.0153 J mol^{-1} K^{-1}, respectively. The free energy of activation, ΔG^* have also been computed at 303 K (Table-3).

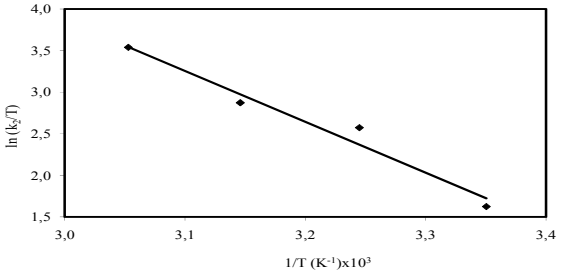

Fig. 10: Plots of $ln(k_2/T)$ versus $1/T$ for adsorption of dye on montmorillonite(Conditions: initial MB 1.0×10^{-4} mol L^{-1}, stirring speed 200 rpm, ionic strength 0 mol L^{-1} NaCl, solution pH 5.95 (Natural)).

Table-3: Thermodynamic parameters of methylene blue adsorption onto montmorillonite

	T (K)			
	303	313	323	333
ΔG* (kJ mol-1)	47.587	47.740	47.893	48.045
ΔH* (kJ mol-1)		42.958		
ΔS* (kJ mol-1 K-1)		-0.0153		

Experimental

Materials

The montmorillonite sample was obtained from Süd-Chemie Processing Plants (Balikesir, Turkey). The chemical composition and physicochemical properties of the montmorillonite found in Turkey were given in Table-4 and Table-5. The montmorillonite sample was treated before using in the experiments as follows: the bulk containing 10 g L^{-1} montmorillonite was mechanically stirred for 24 h. after waiting for about two minutes the supernatant suspension was filtered through a whatman filter paper (Φ = 12.5 cm (diameter of filter paper)). The solid sample was dried at 110 °C for 24 h. and then sieved by 45-90-mesh sieve. The specific surface area of montmorillonite was measured by BET N_2 adsorption.

Table-4: Chemical composition of montmorillonite

Component	Weight (%)
SiO_2	49.40
Al_2O_3	19.70
MgO	0.27
CaO	1.50
Fe_2O_3	0.30
Na_2O	1.50
H_2O	25.67

Table-5: Physicochemical properties of montmorillonite.

Parameters	Value
Color	White
Density (g/cm^3)	2.3 – 3
Transparency	Semi-transparent and opaque
Brightness	Matt
Surface Area(m^2/g)	95.36 m^2/g
Reflective index	1 – 2

All reagents were of analytical grade chemicals. All solutions were prepared with double distilled water. The cationic dye used in this study. MB was purchased from Merck Co., Germany. MB has a molecular weight of 373.9 g mol^{-1} and its chemical formula is $C_{16}H_{18}ClN_3S.3H_2O$ [55]. The structure of MB dye was illustrated in Fig. 11. MB concentration in the sample solution was determined using a spectrophotometer (UNICAM UV-visible spectrophotometer) at a wavelength of 663 nm [20]. Calibration curves were plotted between absorbance and concentration of the dye solution.

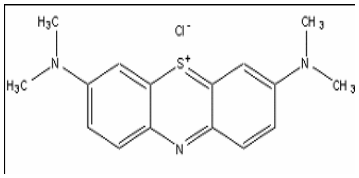

Fig. 11: The structure of methylene blue.

Methods

Kinetic studies were carried out to establish the effect of time on the adsorption process and to quantify the adsorption rate. The effects of agitation speed, initial MB concentration, adsorbent dosage, pH, temperature and ionic strength on the adsorption kinetics were investigated. For the experiments of

adsorption kinetics, 0.3-g-montmorillonite sample was added into a liter of methylene blue solution at desired concentration, temperature and pH. In systems, the dye concentration was 1.0×10^{-4} mol L^{-1}, except those in which the effect of concentration was investigated. Stock solutions of dye (Merck Co. Germany) were prepared in double-distilled water. The pH of the solution was adjusted with 1 mol L^{-1} NaOH or HCl solution by using an Orion 920 A pH-meter with a combined pH electrode.

A preliminary experiment revealed that about 180 min times was required for the adsorption process to reach the equilibrium concentration. A Heidolph RZR 2021 mechanic stirrer at 303 K and 200 rpm for 180 min continuously agitated the mixture. A constant temperature bath was used to keep the temperature constant. Experimental set up was seen Fig. 12. Kinetic experiments were made by using 1000 ml of MB solutions of various concentrations, 5 ml samples were taken at different time intervals and remaining dye concentrations were analyzed. At the end of the adsorption period, the solution was centrifuged for 15 min at 5000 rpm. The samples at appropriate time intervals were taken from the reactor by the aid of the very thin point micropipette, which prevents the transition to solution of montmorillonite samples. Preliminary experiments had shown that the effect of the separation time on the amount of adsorbed dye was negligible. The amounts of dye adsorbed were calculated from the concentrations in solutions before and after adsorption. Each experimental point was an average of two independent adsorption tests [56].

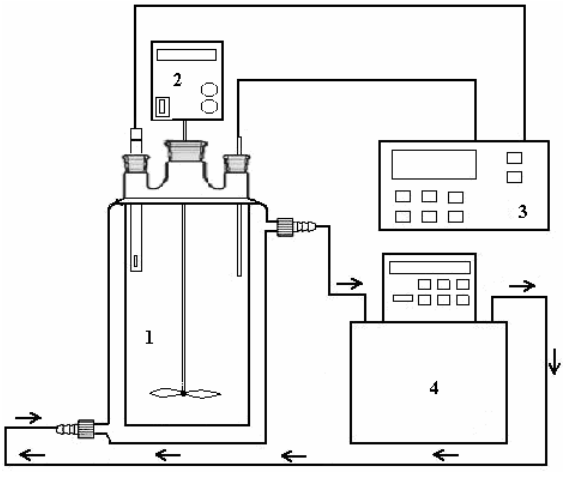

Fig. 12**:** Experimental set up (1. Reactor, 2. Mechanic stirrer, 3. pH-Temperature meter, 4. Circulator).

Following formula was used to determine adsorbed dye concentration *qt*:

$$q_t = \frac{(C_0 - C_t).V}{m} \qquad (1)$$

where *qt (*mol.g^{-1}) is the adsorption capacity at time *t*, *Co* (mol L^{-1}) is the initial dye concentration, *Ct* (mol L^{-1}) is the concentration of dye in solution at time *t*, *V* (L) is the volume, and m (g) is the amount of the adsorbent.

Conclusions

We investigated the adsorption kinetics of MB dye on montmorillonite as a function of contact time, stirring speed, initial dye concentration, adsorbent dosage, ionic strength, pH and temperature; and found that;

1. The adsorption rate of dyes on montmorillonite increased with increase in initial dye concentration, ionic strength, stirring speed, pH and temperature;

2. The intra-particle diffusion was the rate-limiting step for the adsorption process;

3. The diffusion coefficient increased with increase in the stirring speed, ionic strength and temperature; and

4. The activation energy was very low and the process is governed by interactions of physical nature. Montmorillonite can be used for the removal of cationic dyes from aqueous solutions.

Acknowledgements

The authors thank the Balikesir University Research Center of Applied Science (BURCAS).

Nomenclature

C_0	Initial dye concentration in aqueous solution, mol L^{-1}
C_t	Dye concentration in solution at time t, mol L^{-1}
D	Diffusion coefficient, cm^2 s^{-1}
E_a	Activation energy, kJ mol^{-1}
H	Planck's constant
K	Adsorption constant, L g^{-1}
k_b	Boltzmann's constant
k_0	Arrhenius factor, g mol^{-1} min^{-1}
k_1	Adsorption rate constant for pseudo-first-order kinetic equation, min^{-1}
k_2	Adsorption rate constant for pseudo-second-order kinetic equation, g mol^{-1} min^{-1}
k_{0B}	Bang ham's equation constants, ml g^{-1} L
k_{dif}	Intra-particle diffusion rate constant, mol $min^{-1/2}$ g^{-1}
m	Mass of adsorbent, g L^{-1}
pH_{iep}	Isoelectric point
q_e	Equilibrium dye concentration on adsorbent, mol g^{-1}
q_t	The amount of dye adsorbed per unit mass of the adsorbent at time, t, mol g^{-1}

r_0	The radius of the adsorbent particle, cm
R^2	Linear regression coefficient
R_g	Gas constant, J K^{-1} mol^{-1}
S_S	The surface area of adsorbent, m^2 g^{-1}
t	Time, min
T	Temperature, K
$t_{1/2}$	The half-adsorption time of dye, min
V	Solution volume, L
α	Initial adsorption rate in The Elovich equation, mol g^{-1} min^{-1}
β	Desorption constant in The Elovich equation, g mol^{-1}
α_B	Bang ham's equation constants, (less than 1)
β_L	Mass transfer coefficient, m s^{-1}
ΔG^*	Free energy of activation, kJ mol^{-1}
ΔH^*	Enthalpy of activation, kJ mol^{-1}
ΔS^*	Entropy of activation, kJ mol^{-1} K^{-1}

References

1. G. Crini, *Bioresource Technology*, **97**, 1061 (2006).
2. F.-C. Wu and R.-L. Tseng, *Journal of Hazardous Materials*, **152**, 1256 (2008).
3. M. N. V. R. Kumar, T. R. Sridhari, K. D. Bhavani. and P. K. Dutta, *Colorage*, **40**, 25 (1998).
4. K. R. Ramakrishna and T. Viraraghavan, *Water Science and Technology*, **36**, 189 (1997).
5. A. Bozdogan and H. Goknil, *Journal of Natural Sciences Institute of Marmara University*, **4**, p. 83 (1998).
6. K. Majewska-Nowak, T. Winnicki. and J. Wisniewski, *Desalination*, **71**, 127 (1989).
7. O. R. Shendrik, *Kimiyi Technology Vody*, **11**, 467 (1989).
8. Z. Ding, C. W. Min. and W. Q. Hui, *Water Science and Technology*, **19**, 39 (1987).
9. P. Cooper, *Alden Press Oxford*, **9** (1995).
10. S. Wang and H. Li, *Dyes and Pigments*, **72**, 308 (2007).
11. G. Crini, *Dyes and Pigments*, **77**, 415 (2008).
12. M. Dogan, Y. Ozdemir. and M. Alkan, *Dyes and Pigments*, **75**, 701 (2007).
13. S. Wang, Y. Boyjoo, A. Choueib. and Z. H. Zhu, *Water Research*, **39**, 129 (2005).
14. J. J. M. Órfao, A. I. M. Silva, J. C. V. Pereira, S. A. Barata, I. M. Fonseca, P. C. C. Faria. and M. F. R. Pereira, *Journal of Colloid and Interface Science*, **296**, 480 (2006).
15. A. A. Attia, W. E. Rashwan. and S. A. Khedr, *Dyes and Pigments*, **69**, 128 (2006).
16. F. Derbyshire, M. Jagtoyen, R. Andrews, A. Rao, I. Martin-Gullon. and E. Grulke, *Chemistry and Physics of Carbon*, *Marcel Dekker*, *New York*, **27**, 1 (2001).
17. F.-C. Wu, R.-L. Tseng. and R.-S. Juang, *Journal of Hazardous Materials*, **69**, 287 (1999).
18. R. Dolphen, N. Sakkayawong, P. Thiravetyan. and W. Nakbanpote, *Journal of Hazardous Materials*, **145**, 250 (2007).
19. G. Annadurai, L. Y. Ling. and J. F. Lee, *Journal of Hazardous Materials*, **152**, 337 (2008).
20. M. Dogan, M. Alkan, A. Turkyilmaz. and Y. Ozdemir, *Journal of Hazardous Materials*, **109**, 141 (2004).
21. P. Liu and L. Zhang, *Separation and Purification Technology*, **58**, 32 (2007).
22. T. B. Iyim and G. Guclu, *Desalination*, **249**, 1377 (2009).
23. G. McKay, M. El Geundi. and M. M. Nassar, *Process Safety and Environmental Protection*, **74**, 277 (1996).
24. J. X. Lin, S. L. Zhan, M. H. Fang, X. Q. Qian. and H. Yang, *Journal of Environmental Management*, **87**, 193 (2008).
25. N. Dizge, C. Aydiner, E. Demirbas, M. Kobya and S. Kara, *Journal of Hazardous Materials*, **150**, 737 (2008).
26. S. Jain and R. V. Jayaram, *Desalination*, **250**, 921 (2010).
27. A. L. Ahmad, M. M. Loh and J. A. Aziz, *Dyes and Pigments*, **75**, 263 (2007).
28. Y. Guo, S. Yang, W. Fu, J. Qi, R. Li, Z. Wang and H. Xu, *Dyes and Pigments*, **56**, 219 (2003).
29. V. K. C. Lee, J. F. Porter and G. McKay, *Food and Bioproducts Processing*, **79**, 21 (2001).
30. Q. Sun and L. Yang, *Water Research*, **37**, 1535 (2003).
31. V. V. Basava Rao and S. Ram Mohan Rao, *Chemical Engineering Journal*, **116**, 77 (2006).
32. J. German-Heins and M. Flury, *Geoderma*, **97**, 87 (2000).
33. G. Crini, H. N. Peindy, F. Gimbert and C. Robert, *Separation and Purification Technology*, **53**, 97 (2007).
34. S. Karaca, A. Gurses, M. Acıkyıldız and M. Ejder, *Microporous and Mesoporous Materials*, **115**, 376 (2008).
35. T. Robinson, B. Chandran and P. Nigam, *Environment International*, **28**, 29 (2002).
36. Z. Al-Qodah, *Water Research*, **34**, 4295 (2000).
37. S. H. Chien and W. R. Clayton, *Soil Science Society of America Journal*, **44**, 265 (1980).
38. S. Lagergren and B. K. Svenska, *Kungliga Svenska Vetenskapsakademiens Handlingar*, **24**, 1 (1898).
39. Y. S. Ho and G. McKay, *Water Research*, **34**, 735 (2000).
40. Y. S. Ho and G. McKay, *The Canadian Journal of Chemical Engineering*, **76**, 822 (1998).
41. Y. S. Ho and G. McKay, *Trans Institution of Chemical Engineers*, **76B**, 332 (1998).
42. A. Gurses, C. Dogar, M. Yalcın, M. Acıkyıldız, R. Bayrak and S. Karaca, *Journal of Hazardous Materials*, **131**, 217 (2006).

43. A. Al-Futaisi, A. Jamrah and R. Al-Hanai, *Desalination*, **214**, 327 (2007).
44. A. R. Tehrani-Bagha, H. Nikkar, N. M. Mahmoodi, M. Markazi and F. M. Menger, *Desalination*, **266**, 274 (2011).
45. W. J. Weber and J. C. Morris, *Journal Sanitary Engineering Division Proceedings American Society of Civil Engineers*, **89**, 31 (1963).
46. T. Furusawa and J. M. Smith, *Industrial and Engineering Chemistry Fundamental*, **12**, 197 (1973).
47. C. Aharoni, S. Sideman and E. Hoffer, *Journal of Chemical Technology and Biotechnology*, **29**, 404 (1979).
48. O. Abdelwahab, *Egyptian Journal of Aquatic Research*, **33**, 125 (2007).
49. T. Furusawa and J. M. Smith, *AIChE Journal*, **20**, 88 (1974).
50. Y. S. Ho and G. McKay, *Chemical Engineering Journal*, **70**, 115 (1998).
51. K. P. Yadava, B. S. Tyagi, K. K. Panday and V. N. Singh, *Environmental Technology Letters*, **8**, 225 (1987).
52. M. Al-Ghouti, M. A. M. Khraisheh, M. N. M. Ahmad and S. Allen, *Journal of Colloid and Interface Science*, **287**, 6 (2005).
53. K. Laidler and J. H. Meiser, *Houghton Mifflin New York*, p. 852 (1999).
54. H. Nollet, M. Roels, P. Lutgen, P. Van der Meeren and W. Verstraete, *Chemosphere*, **53**, 655 (2003).
55. A. Rodríguez, J. García, G. Ovejero and M. Mestanza, *Journal of Hazardous Materials*, **172**, 1311 (2009).
56. X.-Y. Yang and B. Al-Duri, *Chemical Engineering Journal*, **83**, 15 (2001).